Interaction of the S6 Proline Hinge with N-Type and C-Type Inactivation in Kv1.4 Channels

Glenna C. L. Bett,[†‡] Agnieszka Lis,[‡] Hong Guo,[‡] MiMi Liu,[‡] Qinlian Zhou,[§] and Randall L. Rasmusson[‡§]

[†]Department of Gynecology-Obstetrics, [‡]Department of Physiology and Biophysics, and [§]Department of Biomedical Engineering, Center for Cellular and Systems Electrophysiology, University at Buffalo, Buffalo, New York

Supplementary Data

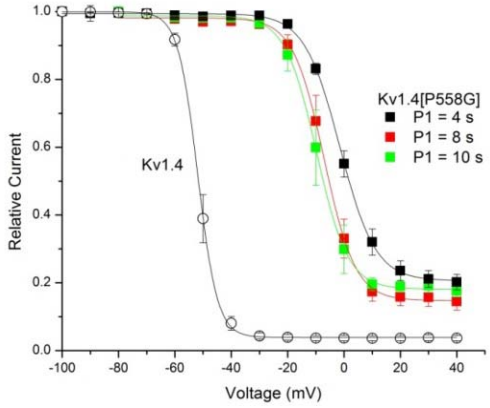

Figure S1. Kv1.4[P558G] steady state inactivation. Kv1.4[P558G] was subjected to a standard two pulse protocol, as shown in Figure 1 of the main paper. The P1 pulse duration was set at 4s, 8s, or 10s, and the degree of steady state inactivation observed in the P2 pulse was calculated as in Figure 4 of the main paper. Increasing the duration of the P2 pulse has little effect on the calculated of degree of inactivation.

Duration P1 Pulse (s)	**V_{half} (mV)**
4	-0.58 ± 2.62
8	-7.06 ± 2.30
10	-9.55 ± 3.10

Table S1: V_{half} of Inactivation. There is no statistically significant difference in V_{half} at 4, 8, and 10 ms ($p>0.1$), however there is a slight trend to a lower V_{half} from 4 s to 8s. The important fact to note is that in all cases there is a statistically and functionally significant rightward shift of V_{half} of Kv1.4[P558G] compared to the V_{half} of Kv1.4. The P1 pulse duration cannot account for this difference. This is similar to the results for the much slower inactivating Kv1.4[P558G]ΔN, where **Figure S2** shows that there is no significant difference in V_{half} for inactivation measured at 5, 8, or 10 s.

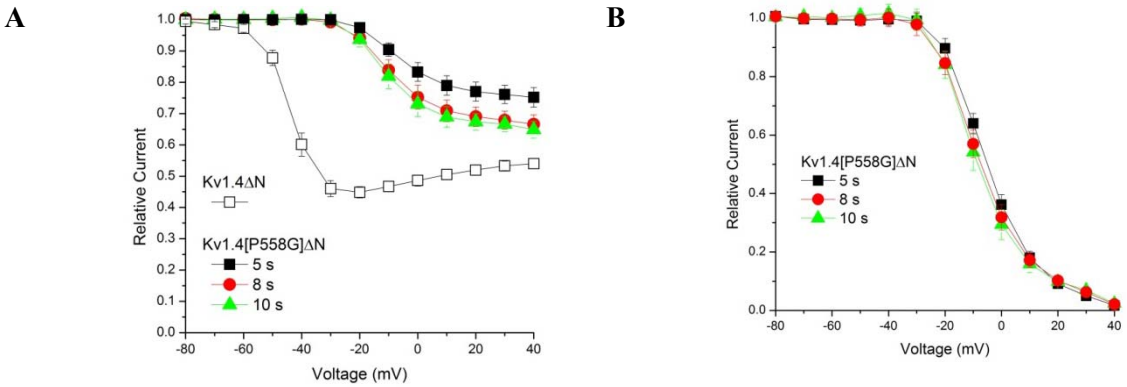

Fig S2. A: Pseudo Steady State Inactivation. A: Inactivation was measured as in Figure 4 of the main paper for Kv1.4ΔN and Kv1.4[P558G]ΔN at 5s, 8s, 10s. **B:** Data from panel A, double normalized to illustrate the similarity in V_{half} of Kv1.4[P558G]ΔN for all pulse lengths (n = 10). There is no significant difference in V_{half} for inactivation measured at 5, 8, or 10 s. However, there is a large functionally and statistically significant shift in the V_{half} of inactivation for Kv1.4[P558G]ΔN at all P1 durations compared to Kv1.4ΔN.

Isochronal Activation.

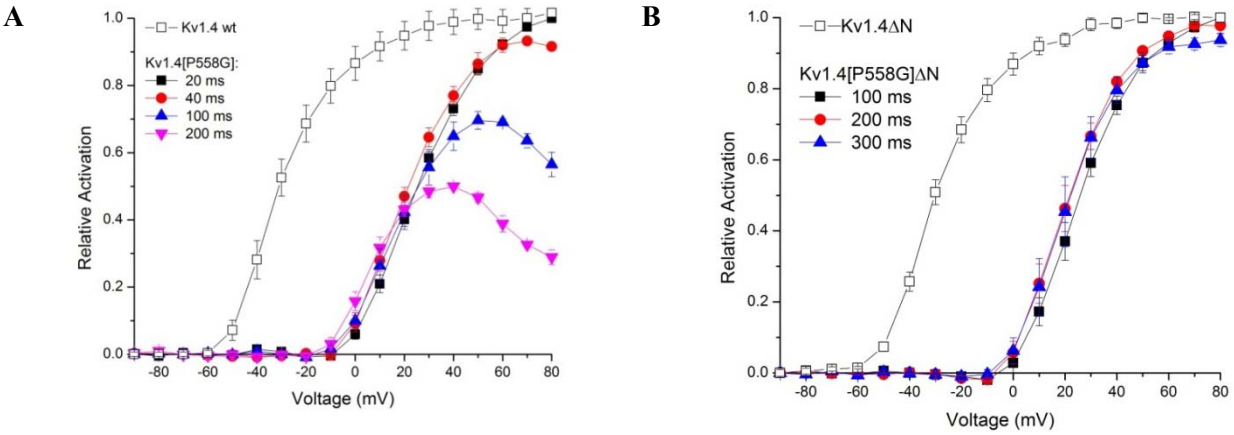

Figure S3. Effect of P1 duration on estimation of V_{half} activation. Oocytes were clamped with an activating pulse of variable duration (as given in the legend) to activate the channel. The second pulse, P2, was to -40 mV, and the peak of the P2 tail current was measured. **A: Kv1.4 and Kv1.4[P558G].** Because activation and inactivation overlapped, the peak tail current elicited by the 20 ms P1 activation pulse to +80mV was used as a normalization value for all tail currents. Pseudo steady-state activation is similar over a broad range of P1 durations. With longer duration activation steps, activation overlap with inactivation becomes considerable. **B: Kv1.4ΔN and Kv1.4[P558G]ΔN.** Activation is similar with depolarization steps of 100, 200 and 300 ms. The peak current elicited by the 100 ms P1 pulse was used as a normalization value. Kv1.4 and Kv1.4ΔN are from Figure 2 in the main paper.

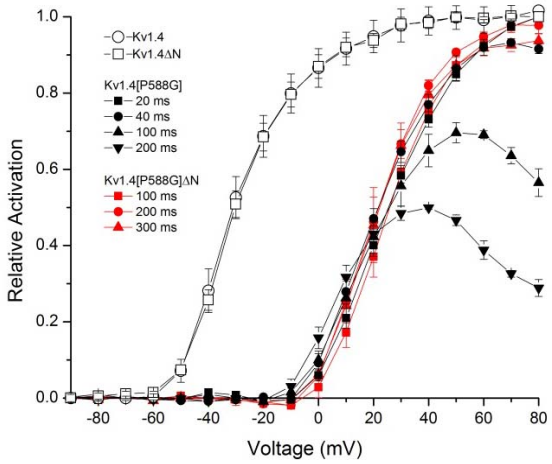

Figure S4: Combined data from **Figure S3 A, B** and main paper **Figure 3 E,F** demonstrating similarities in V_{half} and slope for steady state activation. These results demonstrate that the shift of activation threshold induced by the proline mutations is uninfluenced by differing pulse duration measurements and that the pulse duration cannot account for a functionally significant portion of the observed shift in activation.

A Markov Model of Kv1.4 with pre-activated non-conducting state

We analyzed our existing model of Kv1.4 (1) modified with a primed but non-conducting state connected to the open state by a voltage insensitive step, as suggested by the Bezanilla and Aldrich groups for the last step of opening of the voltage gated Shaker potassium channel (2,3). The structure of this channel is:

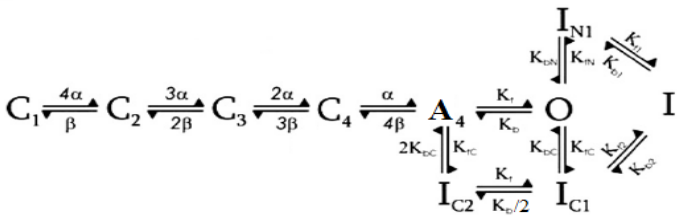

Scheme S1

The relatively fast voltage-dependent activation of Kv1.4 constrains K_f and K_b to be relatively fast. We chose 1 ms forward and 1 ms backward rate constants for this step. Using this model, activation and deactivation are still within the experimental error of measurements by Comer et al (4), as shown in Figure S5.

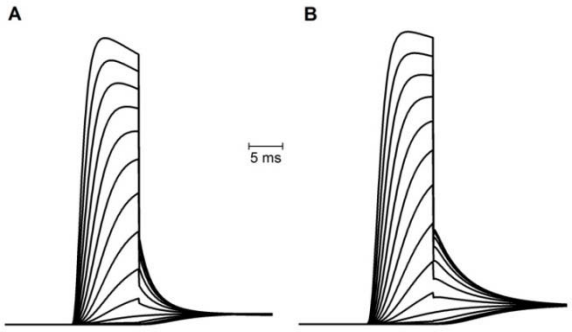

Figure S5. Simulated activation. A 10 ms pulse was applied from the holding potential of -90 to a series of voltages between -90 and + 50 mV. The second pulse was to -50 mV. **A:** Original model (1). **B:** Scheme S1, with activated non-conducting state included.

We used the same protocol used for **Figure 4** of the main paper to simulate inactivation with this model. The simulated inactivation curves for Scheme S1 have some significant quantitative differences compared to the inactivation curves from the original model. Significantly, when the voltage dependence of inactivation is measured, an anomaly arises. As shown in **Figure S6**, inactivation with Scheme S1 is positive relative to the data from the published model (1). In order to be consistent with the voltage dependence of the experimental data, the C-type inactivated state must therefore be coupled to earlier closed states, which go through voltage-dependent transitions to get to the open state.

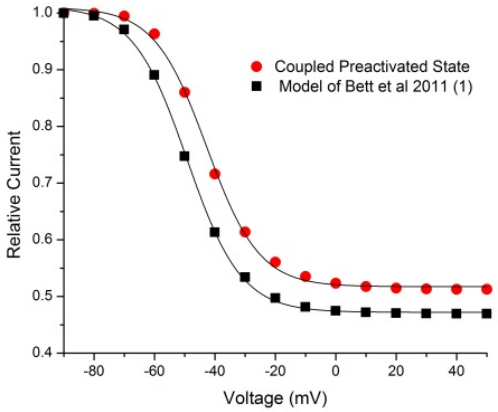

Figure S6. Comparison of inactivation curves for alternative C-type inactivation models. The original inactivation produced by the model of Bett et al 2011 (1) with N-type inactivation removed (■) is shifted to more positive potentials by coupling shown in Scheme S1 which includes a pre-activated non conducting state (●).

These results led us to develop a more complex model with a pre-inactivated state that precedes the activated non-conducting state:

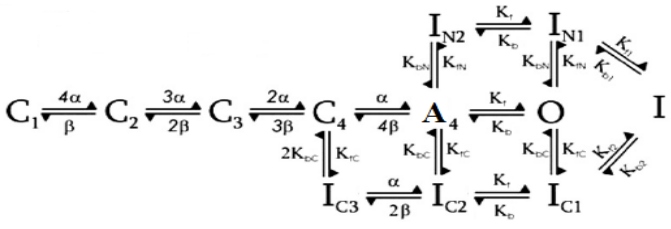

Scheme S2

This model reproduces the basic features already described by the previous paper (1), and enabled us to test putative mechanisms underlying the results presented in the main paper.

We examined whether slowed activation might contribute to the observed slowed inactivation for Kv1.4[P558G]. The model reproduced slowed inactivation when activation was slowed by a factor of 100, but this resulted in a significant delay in peak current which was not observed in the experimental data (**Figure S7**).

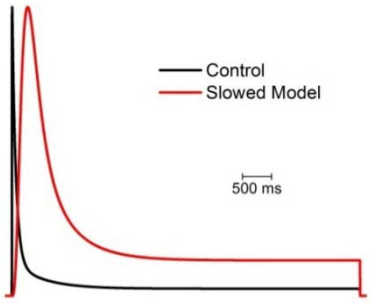

Figure S7. Slowing of inactivation by overlap with slow activation. Apparent slowing of inactivation can be simulated by slowing activation, but requires slowing of activation by ~100 fold. Black line: control. Red line: Activation slowed by 100 fold, normalized to control peak current.

The late rate limiting step of activation

The decreased sigmoidicity and shift of $V_{½}$ of activation with the proline mutations (see Table 1 and Figure 3 Main Paper) suggest that a late rate-limiting cooperative step in the activation of the mutant channels becomes dominant and increases the total energy needed to open the channel. This is consistent with the biophysical mechanisms proposed for the ILT mutations, which slow activation of Shaker channels [3]. The observation that P558G and P558A resulted in activation losing its sigmoidicity and becoming relatively voltage insensitive can be simulated by slowing the transition from the pre-activated non-conducting to the open state (A_4-O), as shown in **Figure S8A**. However, shifting the steady state activation to more positive potentials requires modification of the voltage sensitive steps. Attempts to simulate the slowing of activation by only slowing the voltage dependent steps resulted in noticeable sigmoidicity and a strong voltage dependence (**Figure S8 B**). In summary, in order to reproduce the activation of Kv1.4[P558G]ΔN, we needed to shift the early voltage dependent steps and at the same time make the voltage insensitive transition from the primed state to the open state very slow relative

to activation. This suggests the possibility that earlier voltage-dependent stages of activation and a late cooperative opening are both affected by S6 proline mutations.

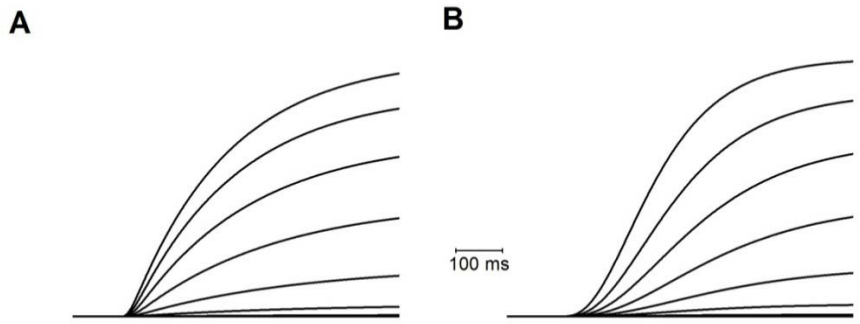

Figure S8. Modeling activation of Kv1.4[P558G]ΔN. **A:** Slowing the voltage insensitive transitions from the pre-activated non conducting state to the open state (A4-O) results in removal of sigmoidicity. **B:** Slowing of the earlier voltage dependent transitions of activation results in significant sigmoid behavior, which is not seen in the experimental data.

Next, we assessed whether the apparent "activation" kinetics of Kv1.4[P558A] might in fact reflect a convolution of fast N-type inactivation superimposed on very slow activation, as occurs over a limited range of voltages for the HERG channel (5). **Figure S9** shows that for a variety of parameter combinations, the simulations do not match the experimental results.

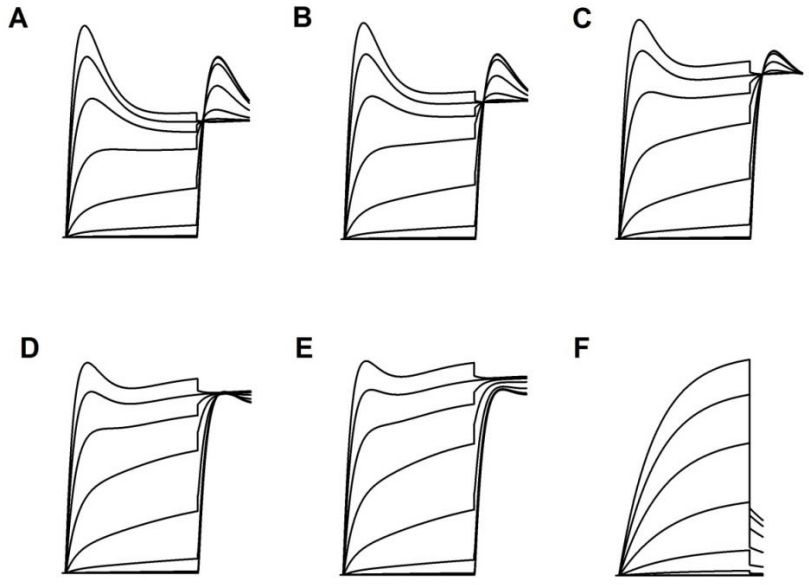

Figure S9. Simulated traces with fast activation superimposed on slow activation. Several different inactivation parameters failed to produce the apparent rapid voltage insensitive activation over a range of potentials although some could mimic fast activation over a limited range. Over larger ranges activation

was biphasic or showed a transient. A family of traces were simulated as an example with the slow activation seen in panel F and coupled inactivation. K_{bN} was reduced to **A:** 0.1 **B:** 0.12 **C:** 0.15 **D:** 0.18 **E:** 0.2 **F:** Slow activation only, with no inactivation

Double Mutant Cycle Analysis

We calculated the free energy of interactions our various constructs for both activation and inactivation from the Boltzmann relationships. These were fit as described in the text for inactivation and for activation using the following function to fit activation curves:

$$(I_{max}/(1+\exp((V-V_{½})/k)))+ C$$

From these fits we obtained k and $V_{½}$. we used the function

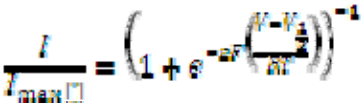

and the Gibbs free energy for activation process is $\Delta G_0 = zFV_{½}$

By combining these two equations, we have the relationship 1/k=zF/RT

Then

$$zF= RT/k$$

So,

$$\Delta G_0=RTV_{½}/k$$

We used this relationship to calculate the free energy difference between closed and open state for activation:

Mutation	Free Energy Difference ΔG (kcal/mol)
Kv1.4	-1.31
Kv1.4ΔN	-1.25
Kv1.4[P558G]	1.41
Kv1.4[P558G]ΔN	1.50

$\Delta\Delta G$ = (ΔG(Kv1.4ΔN) - ΔG(Kv1.4)) - (ΔG(Kv1.4[P558G]ΔN) - ΔG(Kv1.4[P558G])
= -0.02 kcal/mol

Hence $\Delta\Delta G$ showed energy additivity for activation and was essentially insensitive to the presence or absence of the N-terminal.

Analysis of the inactivation relationship following the same analysis yielded:

Mutation	Free Energy Difference

	ΔG (kcal/mol)
Kv1.4	-8.68
Kv1.4ΔN	-6.77
Kv1.4[P558G]	0.15
Kv1.4[P558G]ΔN	0.14

$$\Delta\Delta G = (\Delta G(Kv1.4\Delta N) - \Delta G(Kv1.4)) - (\Delta G(Kv1.4[P558G]\Delta N) - \Delta G(Kv1.4[P558G])$$
$$= 1.92 \text{ kcal/mol}$$

The simplest interpretation of these data is that there is a direct interaction between the P558G mutation and N-terminal ball binding. This type of interaction is consistent with the known interaction domains of N-terminal binding and the S6 domains. The free energy value calculated suggests that this direct interaction provides about: 1.94/(0.16+8.75) = 22% of the total difference in free energy shift of N-type inactivation that is not shared in common with C-type inactivation.

An alternative interpretation is that this free energy difference is likely to be equivalent to the differences introduced in the P558G mutation between the pre-activated non-conducting state and the open state to which C-type and N-type are coupled, respectively. Both of these interpretations are highly speculative given the potential complications arising from the non-true equilibrium nature of some of the measurements and the complexity of the activation process, which is overly simplified by the Boltzmann fit to this data.

Supplementary References

1. Bett, G. C., I. Dinga-Madou, Q. Zhou, V. E. Bondarenko, and R. L. Rasmusson. 2011. A model of the interaction between N-type and C-type inactivation in Kv1.4 channels. Biophys J. 100:11-21.
2. Zagotta, W. N., T. Hoshi, and R. W. Aldrich. 1994. Shaker potassium channel gating. III: Evaluation of kinetic models for activation. Journal of General Physiology 103:321-362.
3. Gagnon, D. G., and F. Bezanilla. 2010. The contribution of individual subunits to the coupling of the voltage sensor to pore opening in Shaker K channels: effect of ILT mutations in heterotetramers. J Gen Physiol. 136:555-568.
4. Comer, M. B., D. L. Campbell, R. L. Rasmusson, D. R. Lamson, M. J. Morales, Y. Zhang, and H. C. Strauss. 1994. Cloning and characterization of an Ito-like potassium channel from ferret ventricle. American Journal of Physiology 267:H1383-H1395.
5. Wang, S., S. Liu, M. J. Morales, H. C. Strauss, and R. L. Rasmusson. 1997. A quantitative analysis of the activation and inactivation kinetics of HERG expressed in Xenopus oocytes. Journal of Physiology 502:45-60.